Original Article

FXR activation suppresses NF-κB signaling, proliferation and migration in cervical cancer cells

Yuanqiang Li[1#], Yangjian Hong[2#], Huize Shen[1], Jingnan Zhou[3], Daniel Cesar[4], José Eleutério Jr[5], Motoki Matsuura[6], Yanyang Liu[2], Cong Luo[7], Qinglin Li[1,2]

[1]Key Laboratory of Integrated Chinese and Western Medicine Oncology, Zhejiang Cancer Hospital, Hangzhou, China; [2]Wenzhou Medical University, Wenzhou, China; [3]Procurement Department, Zhejiang Cancer Hospital, Hangzhou, China; [4]Gynecology Oncology-National Cancer Institute, Rio de Janeiro, Brazil; [5]Department of Women, Children and Adolescent Health, Faculty of Medicine, Federal University of Ceará, Fortaleza, Brazil; [6]Department of Obstetrics and Gynecology, Sapporo Medical University, Sapporo, Japan; [7]Department of Hepato-Pancreato-Biliary & Gastric Medical Oncology, Zhejiang Cancer Hospital, Hangzhou, China

Contributions: (I) Conception and design: Q Li, Y Li; (II) Administrative support: C Luo, J Zhou; (III) Provision of study materials or patients: Q Li; (IV) Collection and assembly of data: Y Liu, Y Hong, H Shen; (V) Data analysis and interpretation: Y Liu, Y Hong, H Shen; (VI) Manuscript writing: All authors; (VII) Final approval of manuscript: All authors.

[#]These authors contributed equally to this work.

Correspondence to: Qinglin Li, PhD. Wenzhou Medical University, No. 268 Academy West Road, Lucheng District, Wenzhou 325035, China; Key Laboratory of Integrated Chinese and Western Medicine Oncology, Zhejiang Cancer Hospital, No. 1 East Banshan Road, Gongshu District, Hangzhou 310022, China. Email: qinglin200886@126.com; Cong Luo, MD. Department of Hepato-Pancreato-Biliary & Gastric Medical Oncology, Zhejiang Cancer Hospital, No. 1 East Banshan Road, Gongshu District, Hangzhou 310022, China. Email: lw939291@126.com; Yanyang Liu, MS. Wenzhou Medical University, No. 268 Academy West Road, Lucheng District, Wenzhou 325035, China. Email: yangyang71777@163.com.

Background: The Farnesoid X receptor (FXR) is a nuclear receptor known for its role in inflammation regulation and tumor suppression in various cancers. However, its functional significance and underlying mechanisms in cervical cancer (CC) remain unclear. The persistent activation of the nuclear factor kappa B (NF-κB) signaling pathway due to inflammation is a key driver of cancer progression. This study investigates the effects of FXR activation in CC and its interaction with the NF-κB pathway.

Methods: CC cells were treated with GW4064, an FXR agonist (3 μM), and xenograft tumor models were assigned to receive 30 mg/kg GW4064. NF-κB-mediated transcriptional activity was assessed using a dual-luciferase reporter assay. Gene expression in CC cells and mouse tissues was analyzed via quantitative real-time polymerase chain reaction (qRT-PCR), while key proteins in the NF-κB and STAT3 signaling pathways were examined using Western blotting. Cell proliferation, migration, and invasion were evaluated through methylthiazolyldiphenyl-tetrazolium bromide (MTT), wound healing, and real-time cellular analysis (RTCA), respectively. Apoptosis was measured using a fluorescein isothiocyanate (FITC) Annexin V Apoptosis Detection Kit I.

Results: FXR deletion in 6- to 8-week-old C57B/6 female mice led to abnormal upregulation of inflammatory genes in the cervix and aberrant NF-κB activation. Treatment with GW4064 suppressed NF-κB-regulated gene expression in Hela and Siha CC cells and inhibited NF-κB activity at the transcriptional level. Mechanistically, FXR activation suppressed tumor necrosis factor alpha (TNFα)-induced phosphorylation of NF-κB inhibitor alpha (IκBα) by directly binding to the promoter of inhibitor of nuclear factor kappa B kinase regulatory subunit gamma (IKBKG), thereby inhibiting its transcription. Additionally, FXR activation reduced CC cell proliferation and migration. In vivo, xenograft experiments in Hela cell-bearing Bagg's albino (BALB/c) nude female mice confirmed that FXR activation significantly suppressed tumor growth.

Conclusions: These findings highlight FXR activation as a potential therapeutic strategy for CC by targeting the NF-κB pathway as shown in both *in vitro* and *in vivo*.

Keywords: Farnesoid X receptor (FXR); GW4064; cervical cancer (CC); nuclear factor kappa B signaling (NF-κB signaling); proliferation

Submitted Mar 06, 2025. Accepted for publication Apr 18, 2025. Published online Apr 27, 2025.
doi: 10.21037/tcr-2025-522
View this article at: https://dx.doi.org/10.21037/tcr-2025-522

Introduction

Cervical cancer (CC) is the fourth most common cancer and the fourth leading cause of cancer-related mortality among women worldwide (1). Annually, approximately 600,000 new cases of CC are diagnosed, with over 300,000 CC-related deaths (2). The high incidence and mortality rates in underdeveloped countries are largely attributed to limited screening programs and low human papillomavirus (HPV) vaccination coverage (3). High-risk HPV is associated with virtually 100% of cases of squamous cell carcinoma of the cervix, and viral persistence is the main risk factor for CC, with additional contributing factors including sexually transmitted infections, smoking, and prolonged use of oral contraceptives (4). In recent decades, CC incidence and mortality rates have declined significantly in most regions due to the widespread implementation of HPV vaccination, CC screening programs, and improvements in genital hygiene (5). However, despite these preventive advances, the recurrence rate of advanced CC remains high (6). Thus, understanding the molecular mechanisms underlying CC progression and identifying novel therapeutic targets remain crucial.

The Farnesoid X receptor (FXR) is a member of the nuclear receptor family and functions as a transcription factor by binding to specific ligands to regulate downstream gene expression (7). Initially, FXR was primarily associated with bile acid, lipid, and energy metabolism (8). Subsequent research has highlighted its crucial role in liver diseases, demonstrating its ability to counteract the development of hepatitis, non-alcoholic fatty liver disease (NAFLD), liver fibrosis, and even hepatocellular carcinoma (9-13). The role of FXR in cancer has been widely studied. In colorectal cancer, cholangiocarcinoma, osteosarcoma, and prostate cancer, FXR exhibits tumor-suppressive effects (14-17). Conversely, in breast cancer, non-small cell lung carcinoma, pancreatic cancer, renal cancer, and thyroid cancer, FXR has been found to be associated with tumor-promoting properties (18-22). However, research on FXR in CC remains limited. Previous studies by our group demonstrated that FXR inhibits hepatitis through suppression of the nuclear factor kappa B (NF-κB) signaling pathway and hinders esophageal cancer progression via the mitogen-activated protein kinase/extracellular signal-regulated kinase (MAPK/ERK) pathway (23,24). Given these findings, we sought to investigate the role of FXR in cervical inflammatory response and CC.

The NF-κB family consists of five members in mammals, with the classical NF-κB signaling pathway involving the p65 (RelA) and p50 (NF-κB1) heterodimer, which interacts with inhibitors of NF-κB (IκB) proteins, such as NF-κB inhibitor alpha (IκBα), in its inactive state (25). Upon stimulation, IκB proteins are phosphorylated by the IκB kinase (IKK) complex, leading to the release of p65/p50 heterodimers, which subsequently regulate downstream gene expression (26). NF-κB is constitutively activated in CC and is significantly associated with the progression of cervical epithelial lesions toward malignancy (27-30). Given its pivotal role in CC progression, NF-κB represents an attractive target for therapeutic intervention.

Highlight box

Key findings

- Farnesoid X receptor (FXR) inhibits the proliferation, migration, and invasion of cervical cancer (CC) cells *in vitro* and promotes apoptosis by suppressing inflammation-induced activation of the nuclear factor kappa B (NF-κB) signaling pathway. Additionally, FXR activation hinders CC progression *in vivo*.

What is known and what is new?

- FXR inhibits hepatic inflammation and hepatocellular carcinoma progression by suppressing NF-κB signaling.
- This study expands the understanding of FXR by investigating on its role in cervicitis and CC.

What is the implication, and what should change now?

- Our findings suggest that FXR activation holds therapeutic potential in CC by modulating the NF-κB pathway as shown in both *in vitro* and *in vivo*.
- FXR activation may represent a novel strategy for preventing and treating cervicitis and CC.

In this study, we aimed to investigate the role of FXR in cervical inflammation and CC, with a particular focus on its potential interaction with the NF-κB signaling pathway. We present this article in accordance with the ARRIVE reporting checklist (available at https://tcr.amegroups.com/article/view/10.21037/tcr-2025-522/rc).

Methods

Reagents and plasmids

GW4064 was purchased from Sigma-Aldrich (St. Louis, MO, USA), and unless otherwise specified, the concentration used was 3 μM. Human tumor necrosis factor alpha (TNFα) and interleukin 6 (IL-6) were purchased from PeproTech (Rocky Hill, NJ, USA). Anti-phosphorylated IκBα (*p*-IκBα) and anti-IκBα (T-IκBα) antibodies were obtained from Cell Signaling Technologies (Danvers, MA, USA). The *FXR* expression vector and the inhibitor of nuclear factor kappa B kinase regulatory subunit gamma (IKBKG) luciferase vector [wild-type (WT) and mutant (MUT)] were constructed in Zhejiang Key Laboratory of Integrated Chinese and Western Medicine Tumor Research; the primers used are shown in Table S1.

Animals

According to the "resource equation" method, a total of 10 mice were used in each experiment, with five mice in the control group and five in the experimental group. These mice were housed in the Animal Experiment Center of Hangzhou Institute of Medicine (HIM), Chinese Academy of Sciences, in a specific pathogen-free animal room. Q.L. serves as the Deputy Director of the Science and Technology Division at the Hangzhou Institute of Medicine, Chinese Academy of Sciences.

To compare the differences in the inflammatory gene in the cervix of the WT and FXR-knockout (KO) mice, 6- to 8-week-old female WT and FXR-KO C57B/6 mice were euthanized. Their cervixes were removed, snap-frozen in liquid nitrogen, and stored at –80 ℃. Euthanasia was performed using a method that would minimize animal suffering. According to the inclusion criteria based on weight, mice weighing less than 18 g or more than 25 g were excluded, resulting in the exclusion of one mouse from each of the control and experimental groups.

To investigate the effect of *FXR* on the tumor growth of the xenograft tumor mice, 4- to 6-week-old BALB/c nude female mice were subcutaneously injected with 5×10^6 Hela cells per mouse. This procedure was carried out by the first investigator, who was blinded to the group allocation. Once the tumors reached a size of 100 mm^3, the mice were randomly assigned to the control and treatment groups by a second investigator using the number table method. The control group was intraperitoneally injected with corn oil every other day, while the treatment group was intraperitoneally injected with GW4064 (30 mg/kg) every other day. The second investigator was the only one aware of the group allocation. Body weight and tumor size were monitored every other day by a third investigator. After 2 weeks, all mice were euthanized by a fourth investigator, and the tumors were excised, photographed, and further analyzed.

To prevent infection or accidental death during the experimental procedures, strict measures were taken to maintain a clean culture environment, ensure a proper diet for the mice, and guarantee the professionalism of the experimental personnel. When tumor size exceeded 1,500 mm^3 or when mice exhibited signs of significant discomfort, timely care was provided, and euthanasia was performed when necessary.

The FXR-KO and WT C57B/6 female mice, as well as BALB/c nude female mice, were purchased from GemPharmatech Co., Ltd. (Nanjing, China) [license no. SCXK (Su) 2023-0009]. All experiments were approved by the Ethics Committee of HIM Animal Experiment Center (license No. AP2024-09-0201) in China and all procedures followed the National Institutes of Health (NIH) guidelines 8th edition, for the care and use of laboratory animals. A protocol was prepared before the study without registration.

Cell culture and transient transfection

The Hela (Catalog No. 1101HUM-PUMC000011) and Siha (Catalog No. 1102HUM-NIFDC00092) human CC cell lines were purchased from the Institute of Basic Medical Sciences of the Chinese Academy of Medical Sciences (Beijing, China). The cells were cultured in complete Roswell Park Memorial Institute (RPMI)-1640 medium, supplemented with 10% (v/v) fetal bovine serum (FBS) and 1% (v/v) antibiotics (100 U/mL penicillin and streptomycin; Thermo Fisher Scientific, Waltham, MA, USA), at 37 ℃ in a humidified atmosphere containing 5% carbon dioxide. To evaluate the anti-inflammatory effects of *FXR* activation, the cells were seeded at a density of 3.2×10^5 into a 6-well cell culture plate for 16 hours before transfection. The cells

were then transfected with the p65 expression vector using Lipofectamine 2000 (Invitrogen, Carlsbad, CA, USA). After 24 hours of incubation, the cells were pretreated with GW4064 for an additional 24 hours and then were subsequently harvested for further analysis.

Dual-luciferase reporter assay

For the luciferase assay, 8.5×10^4 cells were seeded into a 24-well cell culture cluster. The cells were then co-transfected with the phRL-TK plasmid (200 ng/mL), NF-κBX3-LUC plasmid (2,000 ng/mL), p65 expression vector (200 ng/mL), and *FXR* expression plasmid (200 ng/mL) using Lipofectamine 2000. After 24 hours of transfection, the cells were treated with dimethyl sulfoxide (DMSO) or 3 μM of GW4064 for another 24 hours. For the IKBKG-associated luciferase assays, the cells were co-transfected with the phRL-TK plasmid, IKBKG WT or MUT (1,000 ng/mL) plasmid, and *FXR* expression plasmid for 48 hours. The cells were then harvested, and the dual-luciferase reporter assay was performed in accordance with the manufacturer's instructions (Promega, Madison, WI, USA).

RNA isolation and quantitative real-time polymerase chain reaction (qRT-PCR)

Total RNA was isolated from the cells using a TRIZOL reagent (Thermo Fisher Scientific) and transcribed to complementary DNA (cDNA) using the Strand cDNA Synthesis kit (Thermo Fisher Scientific) as described previously (24). qRT-PCR was carried out using the Power SYBR Green PCR Master Mix protocol (Applied Biosystems, San Diego, CA, USA) with specific primers designed to amplify the genes. The primers used for the qRT-PCR are shown in Table S2.

Protein extraction and immunoblot analysis

The CC cells were treated with GW4064 for 24 hours, followed by incubation with TNFα for 1 hour or IL-6 for 6 hours. Subsequently, the cells were harvested for further analysis. The proteins in the cells were extracted as described previously (24). The protein concentration was determined by bicinchoninic acid assay (Beyotime, Shanghai, China). The proteins were then separated by sodium dodecyl sulfate polyacrylamide gel electrophoresis (SDS-PAGE), transferred to 0.2 μm nitrocellulose membranes, and blocked with 5% non-fat milk for 1 hour. The membranes were then blotted with primary antibodies at 4 ℃ overnight and incubated with horseradish peroxidase-labeled goat anti-rabbit secondary antibody. The blots were visualized using the Tanon 5200 system (Tanon, Hangzhou, China). All antibodies used in the experiments are listed in Table S3.

Methylthiazolyldiphenyl-tetrazolium bromide (MTT) assay

To study the inhibitory effect of *FXR* activation on the viability of the CC cells, the cells were seeded into 96-well cell culture plates and treated with GW4064. Next, 10 μL of MTT reagent (5 mg/mL in Phosphate Buffered Saline) was added into the corresponding wells every 24 hours. After 4 hours of incubation, the MTT formazan was extracted by 100 μL DMSO, and the optical density was then measured at 450 nm by spectrofluorimetry.

Wound healing assays

For the wound healing assays, the CC cells were seeded in 24-well plates. After 24 hours, a wound was created by scratching the cell monolayer with a 100-μL pipette tip. The medium was then replaced with incomplete medium containing either DMSO or GW4064. Representative images of cell migration were captured using the light microscopy system.

Cell migration assay

Cell invasion and migration (CIM) were continuously monitored using CIM-plates to assess the invasive capacity of CC cells with the xCELLigence® real-time cellular analysis (RTCA) declustering potential (DP) instrument system (Agilent Technologies Santa Clara, CA, USA). First, 165 μL of culture medium containing FBS was added to the lower chamber of the CIM-plates, and the upper chamber was then assembled with 50 μL of serum-free medium. After 1 hour, a background reading was recorded. Next, the 1×10^4 cells in serum-free medium with GW4064 were added to the upper chamber. The cell index was measured using the RTCA software every 12 hours until the experiment was completed.

Cell apoptosis assay

Cell apoptosis was detected using the fluorescein

isothiocyanate (FITC) Annexin V Apoptosis Detection Kit I (BD Biosciences, Cat. 556547, San Jose, CA, USA) according to the manufacturer's instructions.

Chromatin immunoprecipitation (ChIP)

ChIP assays were performed using an EZ-ChIPTM Assay Kit (17-371, Sigma-Aldrich) following the manufacturer's instructions. Briefly, the Hela and Siha cells were first transfected with *FXR* overexpression plasmids with 3 × Flag tags. After 48 hours, the cells were fixed with 1% paraformaldehyde for 30 minutes, followed by formaldehyde quenching using 0.125 M glycine. The cells were then harvested, lysed using a sodium dodecyl sulfate (SDS) lysis solution, and sonicated. The chromatin fractions were incubated with anti-Flag antibody or normal mouse immunoglobin G overnight at 4 ℃ and then incubated with protein A/G magnetic beads for another 2 hours. After multiple washes and elutions, the DNA was purified using an adsorption column. Both the input DNA and immunoprecipitated DNA were analyzed by qRT-PCR. The target enrichment of immunoprecipitated DNA was calculated as the percentage of the input DNA. The ChIP primer sequences are listed in Table S2.

Statistical analysis

Unless otherwise specified, all the experiments were conducted with three biological replicates. The data were presented as the mean and standard deviation. Statistical analyses were performed using GraphPad Prism (Version 9.0; La Jolla, CA, USA). The student's *t*-test (two-tailed) was used to compare differences between the two groups. A P value less than 0.05 was considered statistically significant.

Results

FXR deficiency promotes cervical inflammation

A large number of pro-inflammatory genes, such as matrix metallopeptidase 2 (*MMP2*), intercellular adhesion molecule 1 (*ICAM-1*), interleukin 10 (*IL-10*), chemokine (C-C motif) ligand 2 (*MCP-1*), *TNF*α, chemokine (*C-X-C motif*) ligand 2 (*CXCL-2*), interleukin 1 beta (*IL-1*β), interleukin 6 (*IL-6*), matrix metallopeptidase 10 (*MMP10*), and matrix metallopeptidase 7 (*MMP7*), were significantly more highly expressed in the cervix of the FXR-KO mice than the cervix of the WT mice (*Figure 1A*). We randomly selected 4 out of 6 mice in each group for western blot experiments, which showed that the levels of *IκBα* and *STAT3* phosphorylation were higher in the cervix of the FXR-KO mice than the cervix of the WT mice (*Figure 1B*).

FXR activation inhibits the proliferation and migration of human CC cells

The MTT assay results showed that the cell proliferation rate of GW4064 treated group (1, 2, and 3 μM) was more inhibited than that of untreated group, and the rate of inhibition was proportional to the concentration of GW4064 (*Figure 2A,2B*). Additionally, the RTCA showed that treatment with GW4064 (3 μM) inhibited the proliferation of the Hela cells (*Figure 2C*). Similarly, the cell scratch assay and RTCA also showed that the invasiveness capacity of the Hela cells and Siha cells decreased after treatment with 3 μM of GW4064 (*Figure 2D-2F*).

Activation of FXR promotes apoptosis in CC cells

Next, we examined the effect of *FXR* activation on CC cell apoptosis. GW4064 (1, 3, and 5 μM) treatment for both 24 and 48 hours promoted the apoptosis of the Hela cells in a dose-dependent manner (*Figure 3A,3B*). In the Siha cells, the GW4064 (1 and 3 μM) treatment for 48 hours had the same effect (*Figure 3C*). Additionally, *FXR* activation (3 μM GW4064 treated) promoted the expression of various pro-apoptotic genes in the Hela cells (*Figure 3D*).

Activation of FXR antagonizes the NF-κB signaling pathway in CC cells

The messenger RNA (mRNA) levels of the NF-κB target genes, such as *MCP-1*, interleukin 1 alpha (*IL-1*α), *ICAM-1*, *TNF*α, interferon-inducible protein-10 (*IP-10*), *IL-6*, *IL-1*β, *MMP2*, and transforming growth factor beta 2 (*TGF*β*2*), were more increased in the TNFα-treated (10 ng/mL) cells than the non-treated control cells (*Figure 4A,4B*). The upregulation of these genes was inhibited by the activation of FXR (3 μM GW4064 treated) (*Figure 4A*). In addition to this, the Hela cells transfected with the p65 plasmid expressed higher mRNA levels of inflammatory factors, including *MCP-1*, inducible nitric oxide synthase (*INOS*), *ICAM-1*, *TNF*α, *IP-10*, and *IL-6* than the untreated cells (*Figure 4B*). In addition, the treatment of GW4064 (3 μM) significantly suppressed the upregulation of these inflammatory factors

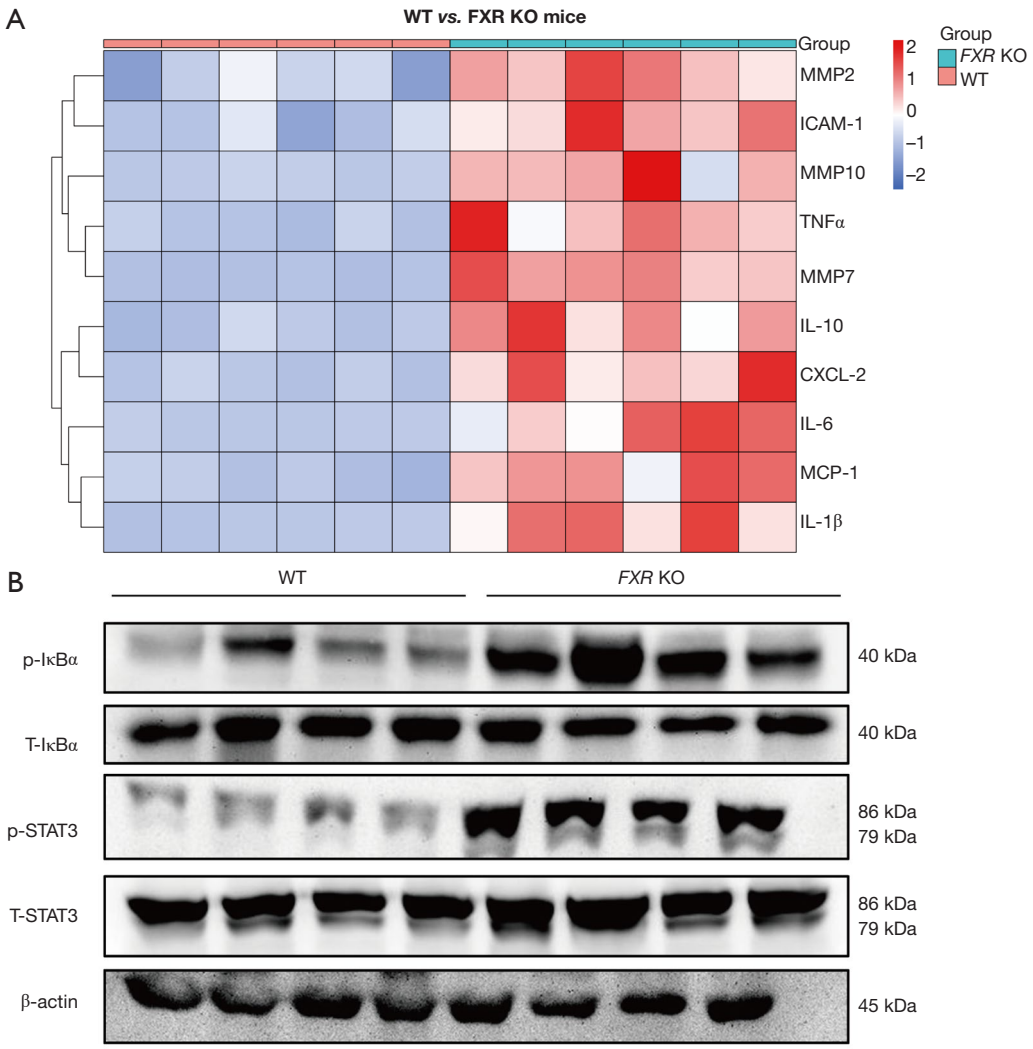

Figure 1 *FXR* deficiency promotes cervical inflammation response. (A) Relative mRNA levels of pro-inflammatory genes in the cervix from the WT and FXR-KO mice, n=6. (B) Western blot showing *p*-IκBα, T-IκBα, *p*-STAT3, and T-STAT3 protein levels in the cervix from the WT and FXR-KO mice. β-actin served as a loading control. *CXCL-2*, chemokine (C-X-C motif) ligand 2; FXR-KO, farnesoid X receptor-knockout; *ICAM-1*, intercellular adhesion molecule 1; *IL-1β*, interleukin 1 beta; *IL-6*, interleukin 6; *IL-10*, interleukin 10; *MCP-1*, chemokine (C-C motif) ligand 2; *MMP2*, matrix metallopeptidase 2; *MMP7*, matrix metallopeptidase 7; *MMP10*, matrix metallopeptidase 10; mRNA, messenger RNA; *p*-IκBα, phosphorylated NF-κB inhibitor alpha; *p*-STAT3, phosphorylated STAT3; T-IκBα, NF-κB inhibitor alpha; T-STAT3, total STAT3; *TNFα*, tumor necrosis factor alpha; WT, wild-type.

(*Figure 4B*), suggesting that activation of FXR antagonized the expression of NF-κB-regulated genes in CC cells. To examine whether *FXR* activation decreased NF-κB-mediated transcriptional activity, luciferase assays were performed. The overexpression of p65 resulted in seven-fold greater NF-κB reporter activity, while NF-κB activity was reduced by GW4064 (3 μM) in the presence of *FXR* (*Figure 4C*), suggesting that activation of FXR inhibited the transcriptional activity of NF-κB. IκBα is a crucial inhibitor of the NF-κB pathway. The phosphorylation of the IκBα proteins by IKK leads to degradation via ubiquitination and subsequently relieves the inhibition of the NF-κB pathway. In the present study, to evaluate the underlying mechanism by which *FXR* acts to suppress the TNFα-

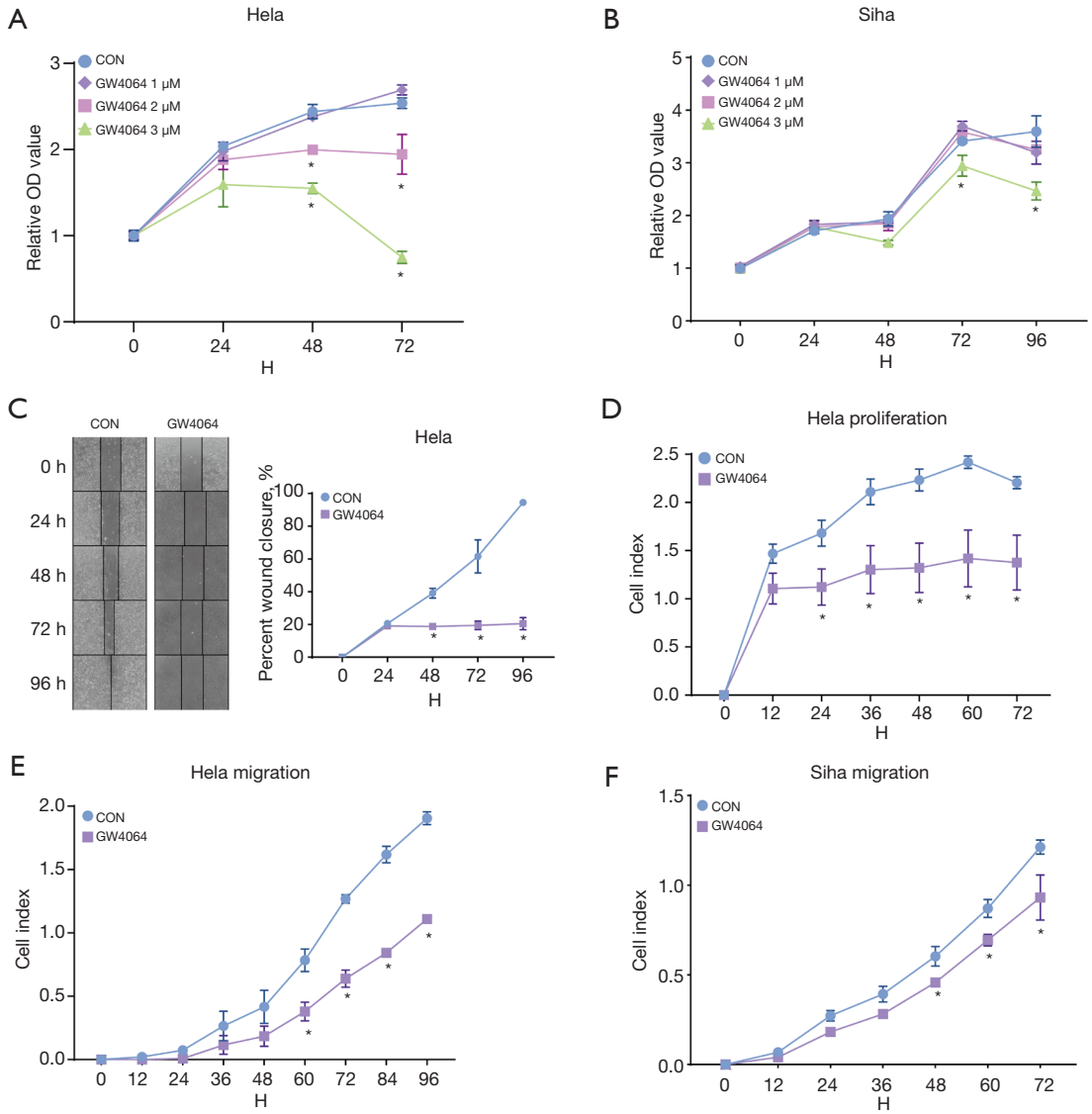

Figure 2 *FXR* activation impairs the proliferation and migration of human CC cells. (A,B) *FXR* activation by GW4064 inhibited the proliferation of the Hela (A) and Siha (B) cells. The proliferation of the cells was analyzed by MTT assay. (C) Left panel: following the activation of *FXR*, the Hela cells exhibited a lower scratch closure rate than the control cells. Magnification: ×40. Right panel: the scratch closure rate was scanned using Image J software. (D) FXR activation by GW4064 inhibited the proliferation of the Hela cells. The proliferation of the cells was analyzed by RTCA. (E,F) *FXR* activation by GW4064 inhibited the migration of the Hela (E) and Siha (F) cells. The migration of cells was analyzed by RTCA. Cell index = (impedance at time point n – impedance in the absence of cells)/nominal impedance value. The value of cell index is positively correlated with the ability of cell proliferation, migration and invasion. *, P<0.05. CC, cervical cancer; CON, control; *FXR*, farnesoid X receptor; MTT, methylthiazolyldiphenyl-tetrazolium bromide; OD, optical density; RTCA, real-time cellular analysis.

induced activation of NF-κB signaling, we examined whether *FXR* antagonized IκBα phosphorylation. As *Figure 4D*,*4E* shows, the phosphorylation of IκBα was significantly increased in the Hela cells and Siha cells treated with TNFα compared to the non-treated cells (*Figure 4D*,*4E*). Conversely, the GW4064 (3 μM) treatment significantly alleviated the IκBα phosphorylation induced by TNFα. The GW4064 treatment also significantly attenuated STAT3 phosphorylation in the Hela cells and Siha cells (*Figure 4D*,*4E*). The activation of *FXR*

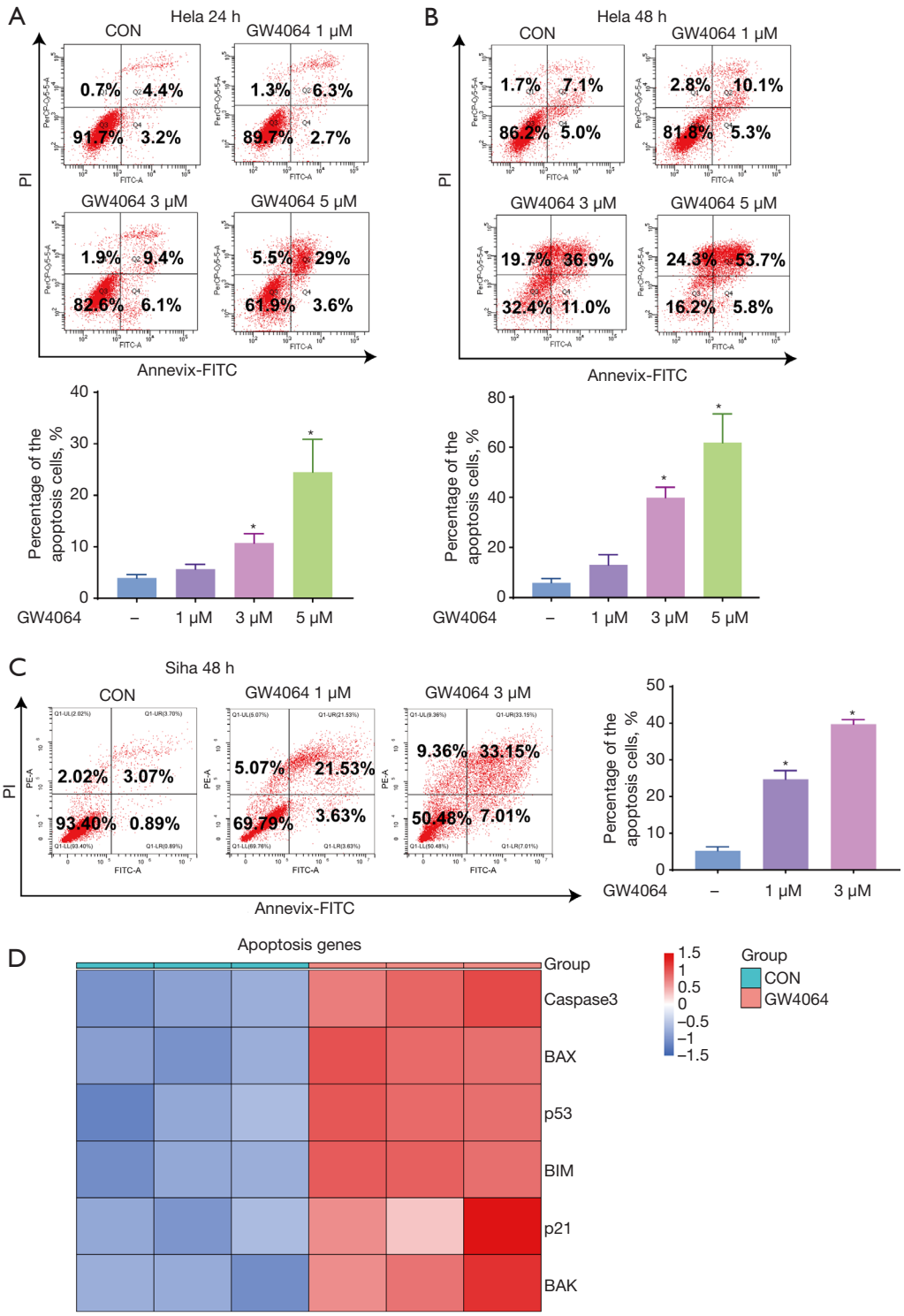

Figure 3 Activation of *FXR* promotes apoptosis in CC cells. (A,B) GW4064 treatment for 24 (A) and 48 (B) hours promoted the apoptosis of Hela cells in a dose-dependent manner, and apoptosis was analyzed using flow cytometry. (C) GW4064 treatment for 48 hours promoted the apoptosis of Siha cells in a dose-dependent manner. (D) Relative mRNA levels of the pro-apoptotic genes in the GW4064-treated Hela cells and control cells. "-": GW4064 untreated group. *, P<0.05. CC, cervical cancer; CON, control; FITC, fluorescein isothiocyanate; *FXR*, farnesoid X receptor; mRNA, messenger RNA; PI, propidium iodide.

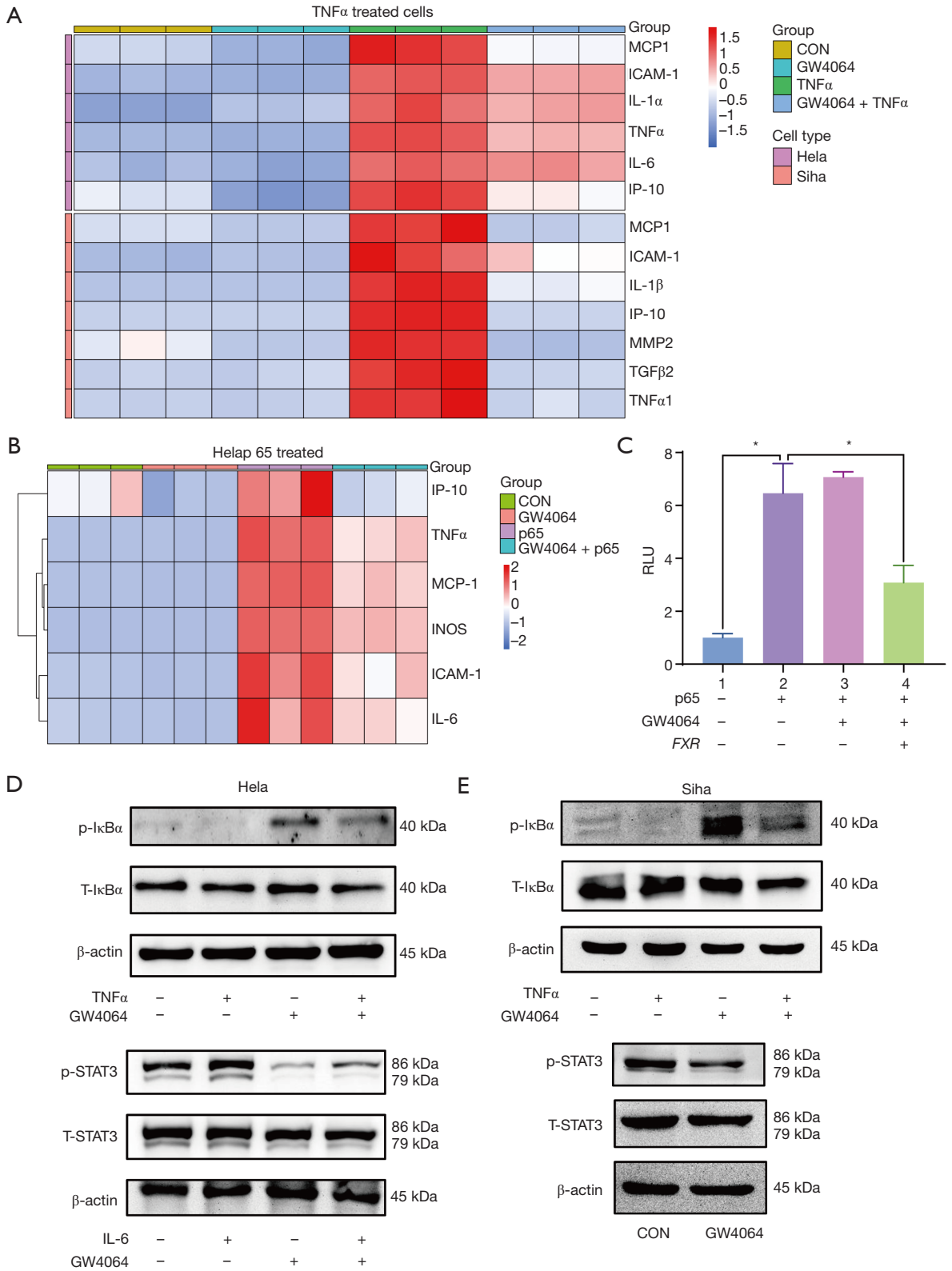

Figure 4 Activation of *FXR* antagonizes the NF-κB signaling pathway in CC cells. (A) Hela and Siha cells were grown in 6-well plates for 16 hours and treated with 3 μM of GW4064 or DMSO for 24 hours, and then stimulated with TNFα (10 ng/mL) for another 1 hour. The cells

were harvested, and the transcript levels of the NF-κB target genes were examined by qRT-PCR. (B) Hela cells were grown in 6-well plates for 16 hours, and transfected with p65 expression vector or control plasmid. After 24 hours of incubation, the cells were treated with 3 μM of GW4064 or DMSO for another 24 hours. The cells were harvested, and the transcript levels of the following cytokines were examined by qRT-PCR. (C) Relative luciferase activities of Hela cells that were co-transfected with the NF-κB reporter plasmid (pNF-κB-Luc), control phRL-TK plasmid, p65 expression plasmid, and *FXR* expression plasmids. The cells were treated with GW4064 (3 μM) or DMSO for 24 hours. (D,E) Representative immunoblots showing *p*-IκBα, T-IκBα, P-STAT3, and T-STAT3 protein levels in the Hela (D) and Siha (E) cells treated with DMSO, TNFα (10 ng/mL), or IL-6 (10 ng/mL), GW4064 (3 μM), TNFα + GW4064. β-actin served as a loading control. *, P<0.05. CC, cervical cancer; CON, control; DMSO, dimethyl sulfoxide; *FXR*, farnesoid X receptor; *ICAM-1*, intercellular adhesion molecule 1; *IL-1α*, interleukin 1 alpha; *IL-1β*, interleukin 1 beta; *IL-6*, interleukin 6; *INOS*, inducible nitric oxide synthase; *IP-10*, interferon-inducible protein-10; *MCP-1*, chemokine (C-C motif) ligand 2; *MMP2*, matrix metallopeptidase 2; mRNA, messenger RNA; NF-κB, nuclear factor kappa B; *p*-IκBα, phosphorylated NF-κB inhibitor alpha; *p*-STAT3, phosphorylated STAT3; qRT-PCR, quantitative real-time polymerase chain reaction; RLU, relative light unit; T-IκBα, NF-κB inhibitor alpha; T-STAT3, total STAT3; *TGFβ2*, transforming growth factor beta 2; *TNFα*, tumor necrosis factor alpha.

antagonized the NF-κB signaling pathway in CC cells.

FXR antagonizes the NF-κB signaling pathway by inhibiting IKBKG transcription

We further explored the mechanism by which *FXR* regulates IκBα phosphorylation. First, qRT-PCR results showed that activation of FXR (3 μM GW4064 or 10 μM 6-eCDCA treated) significantly suppressed the expression of IKBKG, an IκBα upstream gene, in CC cell lines (*Figure 5A*). Next, we used the online tool Nubiscan (https://www.nubiscan.unibas.ch/) to predict whether there are *FXR* binding sites on the IKBKG promoter. As *Figure 5B* shows, there were *FXR* binding sites on the IKBKG promoter (–1,082 to –1,066: 5' GGATCACCTGAGGTCA 3'). We cloned the IKBKG promoter region (–1,220 to –790) into the pGL4.23 plasmid (WT) and investigated the effect of FXR on IKBKG transcriptional activity by luciferase assay. *FXR* overexpression significantly inhibited luciferase expression, indicating that *FXR* bound to the IKBKG promoter and repressed IKBKG transcription (*Figure 5C*). Moreover, after we mutated the *FXR* binding site on the WT plasmid and constructed the MUT plasmid, the inhibitory effect of *FXR* on luciferase expression was eliminated, which further supports this conclusion (*Figure 5D*). In addition, the results of ChiIP experiments showed that the flag antibody significantly enriched the *FXR* binding region on the IKBKG promoter, further showing the binding between *FXR* and IKBKG promoter (*Figure 5E*).

Activation of FXR inhibits CC progression in vivo

Next, we used a nude xenograft mouse model to explore the effect of *FXR* on CC progression *in vivo*. After the GW4064 (30 mg/kg) injection, the size, growth rate, and weight of the subcutaneous tumors in the nude mice were significantly lower than those in the control group (*Figure 6A-6C*). There was no difference in body weight between the two groups of nude mice, indicating that the intraperitoneal injection of GW4064 did not have any significant toxic side effects (*Figure 6D*). In addition, we extracted RNA from the tumors to examine the expression of the inflammation-related genes. As *Figure 6E* shows, the expression of multiple inflammatory genes in the tumors was significantly downregulated after the GW4064 injection. Similarly, the levels of IL-6, IL-1β, and TNFα in the tumor were detected using enzyme-linked immunosorbent assay (ELISA), and there was a significant decrease in the levels of these three inflammatory factors in the tumor after the activation of *FXR* by GW4064 injection (*Figure 6F*). Thus, the activation of *FXR* inhibited the progression of CC *in vivo*.

Discussion

Chronic inflammation is a well-established driver of cancer development, with NF-κB playing a central role in this process. Inflammatory responses activate the NF-κB pathway, promoting the transcription of pro-inflammatory cytokines (e.g., TNFα, IL-6) and chemokines (e.g., IL-8, MCP-1, IP-10), which, in turn, further activates NF-κB, creating a self-perpetuating cycle of inflammation (31). FXR, a nuclear receptor, has been shown to reduce inflammatory responses and cytokine expression in the liver and gastrointestinal tract *in vitro* and *in vivo* (8,32). Additionally, FXR overexpression suppresses CC by inhibiting p53 ubiquitination (33,34), but its broader role in CC progression remains unclear.

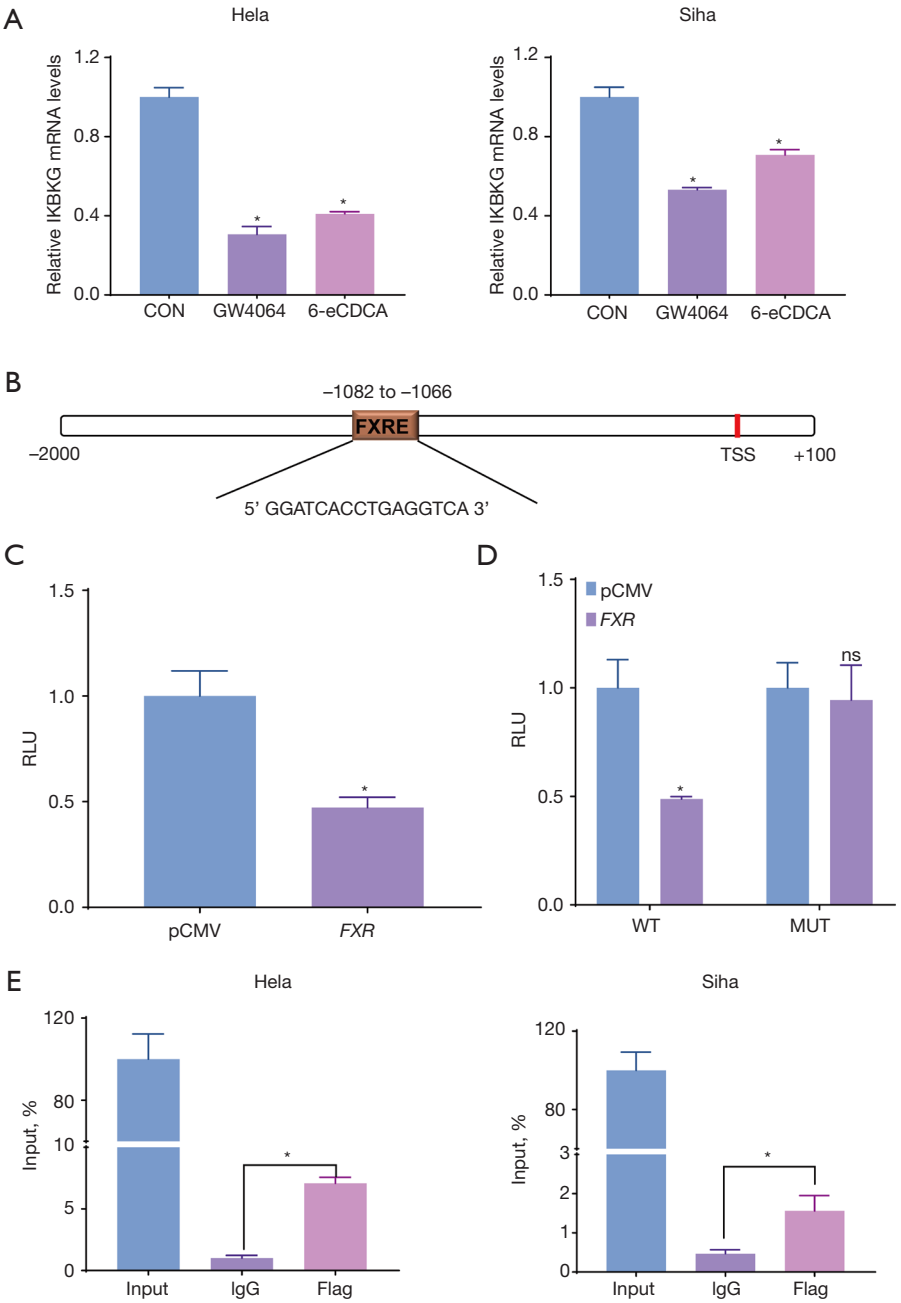

Figure 5 *FXR* antagonizes the NF-κB signaling pathway by inhibiting IKBKG transcription. (A) Relative mRNA levels of IKBKG in GW4064 or 6-eCDCA treated Hela and Siha cells. (B) The online tool NUBIS can predicted the binding site of *FXR* on the IKBKG promoter. (C) Relative luciferase activities of the Hela cells that were co-transfected with the IKBKG reporter plasmid (WT), control phRL-TK plasmid, and *FXR* expression plasmids. (D) Relative luciferase activities of the Hela cells that were co-transfected with the IKBKG reporter plasmid (WT) or mutant IKBKG reporter plasmid (MUT), control phRL-TK plasmid, and *FXR* expression plasmids. (E) Hela and Siha cells were pre-transfected with Flag-tagged *FXR* overexpression plasmids, followed by ChIP with anti-Flag antibodies to confirm the interaction between *FXR* and the IKBKG promoter. *, P<0.05; ns, no significance. ChIP, chromatin immunoprecipitation; CON, control; *FXR*, farnesoid X receptor; *FXRE*, farnesoid X-receptor-responsive element; IgG, immunoglobulin G; IKBKG, inhibitor of nuclear factor kappa B kinase regulatory subunit gamma; MUT, mutant; mRNA, messenger RNA; NF-κB, nuclear factor kappa B; pCMV, control vector; RLU, relative light unit; TSS, transcription start site; WT, wild-type.

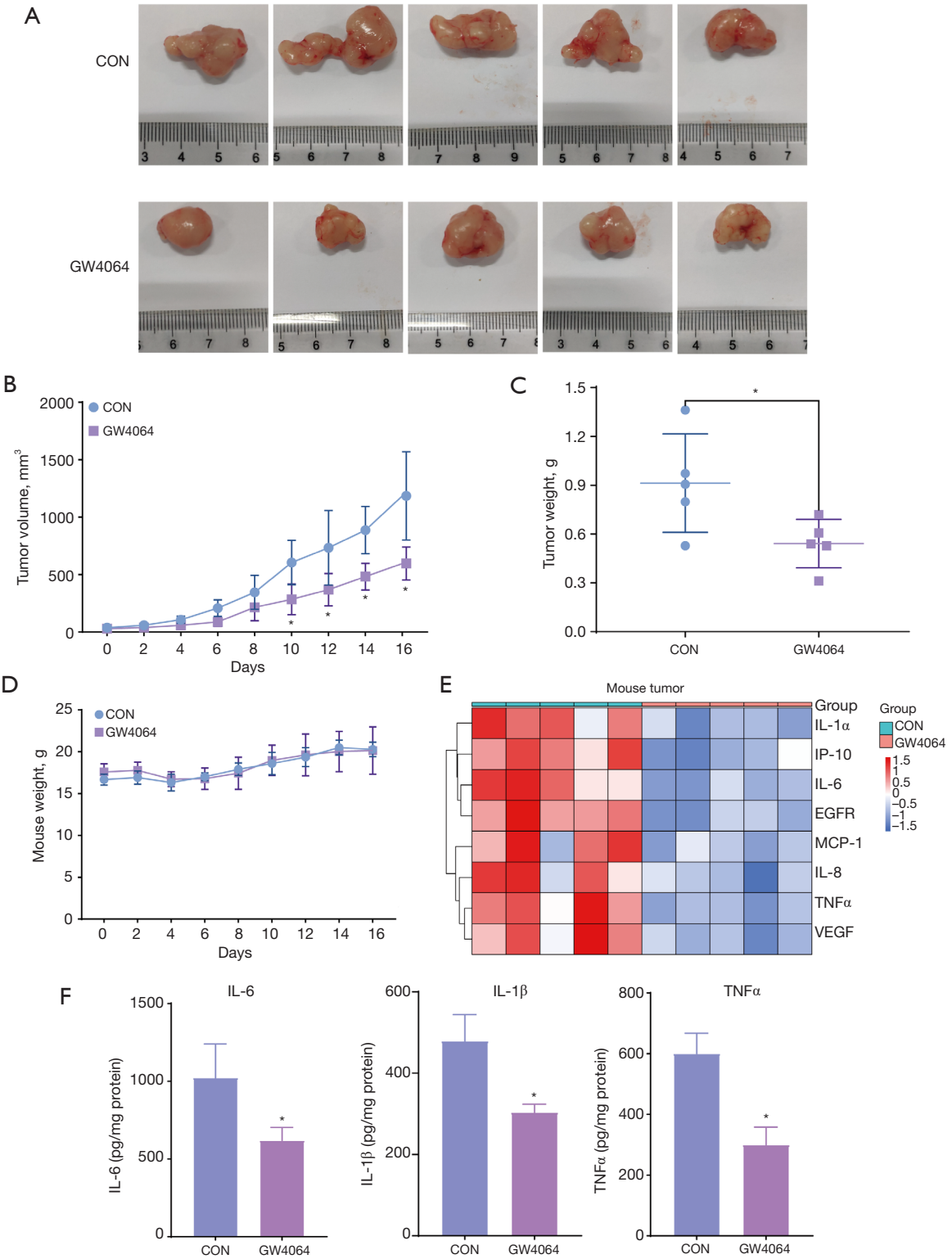

Figure 6 Activation of *FXR* inhibits CC progression *in vivo*. Nude mice were subcutaneously inoculated with Hela cells and then intraperitoneally injected with GW4064 (30 mg/kg) or the vehicle (n=5). (A) Photographs of tumors in the GW4064-treated and control groups. (B) Tumor growth curve. (C) Statistics of tumor weight. (D) Body weight change curve of mice after GW4064 injection. (E)

Relative mRNA levels of pro-inflammation genes in GW4064-treated tumors and control tumors. (F) The levels of IL-6, IL-1β and TNFα in GW4064-treated and control tumors were detected using ELISA assays. n=5. *, P<0.05. CC, cervical cancer; CON, control; EGFR, epidermal growth factor receptor; ELISA, enzyme-linked immunosorbent assay; *FXR*, farnesoid X receptor; IL-1α, interleukin 1 alpha; IL-1β, interleukin 1 beta; IL-6, interleukin 6; IL-8, interleukin 8; IP-10, interferon-inducible protein-10; MCP-1, chemokine (C-C motif) ligand 2; mRNA, messenger RNA; TNFα, tumor necrosis factor alpha; VEGF, vascular endothelial growth factor.

To clarify the effect of FXR activation on NF-κB transcriptional activity, we explored three perspectives. First, the expression of NF-κB downstream genes was detected using qRT-PCR, which was used to assess the activation of NF-κB signaling. Second, luciferase assays were performed using the NF-κB reporter plasmid. There are multiple p65 binding sites on the reporter plasmid. When NF-κB is activated, p65 will bind to the reporter plasmid and induce luciferase expression, therefore the activation of NF-κB can be clarified based on the luciferase activity. Finally, we examined the phosphorylation level of IκBα, a key protein of the NF-κB pathway, by western blot to clarify the activation of NF-κB. Our findings demonstrated that FXR activation via GW4064 repressed NF-κB target genes, downregulated NF-κB-regulated inflammatory factors, and significantly inhibited NF-κB transactivity *in vitro*. These results suggest that FXR may protect against CC by mitigating NF-κB-driven cervical inflammation, consistent with its protective role in colorectal cancer, hepatic cancer, atherosclerosis, and hypertension (8,35-37).

In the classical NF-κB pathway, IκBα is phosphorylated at Ser32 and 36 residues by transforming growth factor β-activated kinase 1 (TAK1)-activated inhibitor of kappa B kinase (IKKβ) in the presence of inflammatory stimulation (38), then IKKβ followed by ubiquitination and subsequent degradation through the 26S proteasome (39), thus the liberated NF-κB, typically the p50/p65 complex, translocates from the cytoplasm to the nucleus and binds to the promoter region of target genes to activate their transcription. This process requires the involvement of at least one non-catalytic accessory protein, such as NF-κB essential modulator (NEMO), in addition to IKK (40). IKKγ, encoded by the IKBKG, acts as a NEMO and is indispensable in the activation of NF-κB signaling (41). The enhancement of IKK and NEMO or proteasome activity, or the deletion or lower expression of nuclear factor of kappa light polypeptide gene enhancer in B-cells inhibitor alpha (*NFKBIA*), which encodes IκBα, participates in the continuous activation of the NF-κB pathway and induces the pathogenesis of malignant tumors (42-44).

Previous studies have shown that high-risk HPV infection activates NF-κB, which in turn creates a chronic inflammatory state (45-47). Precancerous lesions develop with ongoing HPV infection, and may eventually result in tumor development (29). In CC progression, NF-κB is constitutively activated and the overexpression of NF-κB is significantly associated with the progression of cervical epithelial lesions toward CC (27,28). In the current study, we found that *FXR* bound to the IKBKG promoter and suppressed its transcriptional activity leading to reduced TNFα-induced phosphorylation of IκBα at the protein level. This suggests that the decreased production of pro-inflammatory cytokines observed in CC cells treated with an *FXR* agonist may be mediated by lower *p*-IκBα levels. Interestingly, the western blot results showed that *p*-IκBα in Siha cells showed two bands, whereas there was only one band in Hela cells, the phenomenon suggests that there may be a different *p*-IκBα phosphorylation modification site or a different variant of *p*-IκBα in Siha than in Hela.

Because of its crucial role in regulating the metabolism of bile acids, lipids, and glucose, *FXR* has been a promising therapeutic target for cholestatic liver diseases, such as primary biliary cholangitis (PBC) and primary sclerosing cholangitis (PSC), as well as for metabolic liver diseases, especially NAFLD, in the past decades (20,48). The *FXR* agonist obeticholic acid (OCA) was the first drug approved for use in PBC as a second-line treatment for patients unresponsive to ursodeoxycholic acid (UDCA) (49). OCA has been shown to significantly reduce biomarkers associated with PBC, including alkaline phosphatase, bilirubin, aspartate aminotransferase, and alanine aminotransferase (49-51). *FXR* agonists such as OCA (52), cilofexor (53), tropifexor (54), and vonafexor (55) have also demonstrated clinical efficacy in the treatment of NAFLD. Their activation of *FXR* significantly ameliorates steatohepatitis and hepatic fibrosis, reducing liver enzymes and liver fat in patients. In addition, *FXR* has a mitigating effect on inflammatory bowel disease. Activated *FXR* reduces the loss of cuprocytes, protects the intestinal barrier, and inhibits the inflammatory response (56). In the present study, we explored the effect of *FXR* on the inflammatory response of the cervix. Knockdown of *FXR* promoted the

inflammatory response of the cervix, and activation of *FXR* using GW4064 significantly suppressed the expression of inflammatory genes in the cervix. As a potent and selective agonist of *FXR*, GW4064 has great potential in the treatment of metabolic-related diseases of the digestive system and cervical inflammatory conditions, however, problems posed by the structure of GW4064 severely limit its clinical translation. As a non-steroidal agonist of FXR, GW4064 is an isoxazole-based small molecule compound. Its stilbene functionality is a potentially toxic pharmacophore and this also contributes to its nature of ultraviolet (UV) light instability (57). Furthermore, low bioavailability due to its lipophilic/amphiphilic properties and limited plasma exposure due to its high clearance also limit GW4064 clinical translation (58). Currently, the development of *FXR* agonists with high bioavailability and safety based on the modification of the GW4064 structure is a hot research topic (59). Some efficient agonists of FXR have been obtained by somatic replacement of the stilbene functionality or modification of the isoxazole backbone, overcoming some of the issues with GW4064 (59,60). Among them, PX20606 (59) and LJN452 (61) have been evaluated for safety in phase I studies and are currently undergoing clinical phase 2 trials for the treatment of non-alcoholic steatohepatitis (NASH).

The proliferation and migration capacity of tumor cells are key indicators for evaluating tumor malignancy (62). A recent study reported that another *FXR* agonist, OCA, caused cell cycle arrest and suppressed the invasion and migration of human hepatocellular carcinoma cells by interfering with the IL-6/STAT3 signaling pathway (63). In addition, the activation of *FXR* upregulates the expression of the tumor suppressor caudal-related homeobox transcription factor 2 (CDX2), thereby inhibiting the proliferation and migration of colorectal cancer cells *in vivo* and *in vitro* (64). In bladder cancer, activation of FXR by GW4064 inhibits bladder cancer migration and invasion through the down-regulation of cathepsin B and MMP2 (65). These findings further showed the anticarcinogenic function of *FXR* in the pathogenesis of these human cancers. In the present study, we examined whether the activation of *FXR* inhibited the progression of CC. We found that the *in vitro* activation of *FXR* by GW4064 inhibited the proliferation and migration ability of the CC cells and promoted the apoptosis of the CC cells. Similarly, the activation of *FXR* also inhibited tumor growth in the Hela cell-bearing mice *in vivo*. Therefore, activating endogenous *FXR* with its agonists or synthetic derivatives of bile acids could be a promising therapeutic strategy for the prevention and treatment of CC; however, the extent to which the antitumorigenic role of *FXR* contributes to the prevention effect and the potential side effect of these compounds are yet to be explored, and extensive preclinical and clinical studies are needed, which will be our future work.

Conclusions

Our results show that FXR negatively regulates CC by inhibiting NF-κB activation driven by inflammation. Further *in vivo* studies are needed to evaluate the safety and effectiveness of FXR ligands. These findings support the potential of FXR activation as a novel strategy for preventing and treating cervical inflammatory response and CC.

Acknowledgments

None.

Footnote

Reporting Checklist: The authors have completed the ARRIVE reporting checklist. Available at https://tcr.amegroups.com/article/view/10.21037/tcr-2025-522/rc

Data Sharing Statement: Available at https://tcr.amegroups.com/article/view/10.21037/tcr-2025-522/dss

Peer Review File: Available at https://tcr.amegroups.com/article/view/10.21037/tcr-2025-522/prf

Funding: This project was funded by the Zhejiang Province Basic Public Welfare Research Program (No. LGF22H160084 to C.L.), the Zhejiang Province Medical and Health Science and Technology Plan (No. 2023KY615 to J.Z.), and the Cultivation Fund of the National Natural Science Foundation of Zhejiang Cancer Hospital (No. PY2023008 to Yuanqiang Li).

Conflicts of Interest: All authors have completed the ICMJE uniform disclosure form (available at https://tcr.amegroups.com/article/view/10.21037/tcr-2025-522/coif). The authors have no conflicts of interest to declare.

Ethical Statement: The authors are accountable for all

aspects of the work in ensuring that questions related to the accuracy or integrity of any part of the work are appropriately investigated and resolved. All experiments were approved by the Ethics Committee of HIM Animal Experiment Center (license No. AP2024-09-0201) in China and all procedures followed the National Institutes of Health (NIH) guidelines 8th edition for the care and use of laboratory animals.

References

1. Bedell SL, Goldstein LS, Goldstein AR, et al. Cervical Cancer Screening: Past, Present, and Future. Sex Med Rev 2020;8:28-37.
2. Bray F, Laversanne M, Sung H, et al. Global cancer statistics 2022: GLOBOCAN estimates of incidence and mortality worldwide for 36 cancers in 185 countries. CA Cancer J Clin 2024;74:229-63.
3. de Martel C, Plummer M, Vignat J, et al. Worldwide burden of cancer attributable to HPV by site, country and HPV type. Int J Cancer 2017;141:664-70.
4. Johnson CA, James D, Marzan A, et al. Cervical Cancer: An Overview of Pathophysiology and Management. Semin Oncol Nurs 2019;35:166-74.
5. Liu Y, Ai H. Comprehensive insights into human papillomavirus and cervical cancer: Pathophysiology, screening, and vaccination strategies. Biochim Biophys Acta Rev Cancer 2024;1879:189192.
6. Das S, Babu A, Medha T, et al. Molecular mechanisms augmenting resistance to current therapies in clinics among cervical cancer patients. Med Oncol 2023;40:149.
7. Forman BM, Goode E, Chen J, et al. Identification of a nuclear receptor that is activated by farnesol metabolites. Cell 1995;81:687-93.
8. Wang YD, Chen WD, Moore DD, et al. FXR: a metabolic regulator and cell protector. Cell Res 2008;18:1087-95.
9. Yang F, Huang X, Yi T, et al. Spontaneous development of liver tumors in the absence of the bile acid receptor farnesoid X receptor. Cancer Res 2007;67:863-7.
10. Fiorucci S, Antonelli E, Rizzo G, et al. The nuclear receptor SHP mediates inhibition of hepatic stellate cells by FXR and protects against liver fibrosis. Gastroenterology 2004;127:1497-512.
11. Mudaliar S, Henry RR, Sanyal AJ, et al. Efficacy and safety of the farnesoid X receptor agonist obeticholic acid in patients with type 2 diabetes and nonalcoholic fatty liver disease. Gastroenterology 2013;145:574-82.e1.
12. Zhang L, Chen J, Yang X, et al. Hepatic Zbtb18 (Zinc Finger and BTB Domain Containing 18) alleviates hepatic steatohepatitis via FXR (Farnesoid X Receptor). Signal Transduct Target Ther 2024;9:20.
13. Zheng C, Wang L, Zou T, et al. Ileitis promotes MASLD progression via bile acid modulation and enhanced TGR5 signaling in ileal CD8(+) T cells. J Hepatol 2024;80:764-77.
14. Miyazaki T, Shirakami Y, Mizutani T, et al. Novel FXR agonist nelumal A suppresses colitis and inflammation-related colorectal carcinogenesis. Sci Rep 2021;11:492.
15. Liu J, Tong SJ, Wang X, et al. Farnesoid X receptor inhibits LNcaP cell proliferation via the upregulation of PTEN. Exp Ther Med 2014;8:1209-12.
16. Wu B, Xing C, Tao J. Upregulation of microRNA-23b-3p induced by farnesoid X receptor regulates the proliferation and apoptosis of osteosarcoma cells. J Orthop Surg Res 2019;14:398.
17. Chen W, Xu H, Guo L, et al. Role of ACSL4 in modulating farnesoid X receptor expression and M2 macrophage polarization in HBV-induced hepatocellular carcinoma. MedComm (2020) 2024;5:e706.
18. Absil L, Journé F, Larsimont D, et al. Farnesoid X receptor as marker of osteotropism of breast cancers through its role in the osteomimetism of tumor cells. BMC Cancer 2020;20:640.
19. You W, Chen B, Liu X, et al. Farnesoid X receptor, a novel proto-oncogene in non-small cell lung cancer, promotes tumor growth via directly transactivating CCND1. Sci Rep 2017;7:591.
20. Lee JY, Lee KT, Lee JK, et al. Farnesoid X receptor, overexpressed in pancreatic cancer with lymph node metastasis promotes cell migration and invasion. Br J Cancer 2011;104:1027-37.
21. Huang S, Hou Y, Hu M, et al. Clinical significance and oncogenic function of NR1H4 in clear cell renal cell carcinoma. BMC Cancer 2022;22:995.
22. Giaginis C, Tsoukalas N, Alexandrou P, et al. Clinical significance of farnesoid X receptor expression in thyroid

neoplasia. Future Oncol 2017;13:1785-92.
23. Wang YD, Chen WD, Wang M, et al. Farnesoid X receptor antagonizes nuclear factor kappaB in hepatic inflammatory response. Hepatology 2008;48:1632-43.
24. Feng Q, Zhang H, Yao D, et al. Activation of FXR Suppresses Esophageal Squamous Cell Carcinoma Through Antagonizing ERK1/2 Signaling Pathway. Cancer Manag Res 2021;13:5907-18.
25. Hoesel B, Schmid JA. The complexity of NF-κB signaling in inflammation and cancer. Mol Cancer 2013;12:86.
26. Zandi E, Rothwarf DM, Delhase M, et al. The IkappaB kinase complex (IKK) contains two kinase subunits, IKKalpha and IKKbeta, necessary for IkappaB phosphorylation and NF-kappaB activation. Cell 1997;91:243-52.
27. DA Costa RM, Bastos MM, Medeiros R, et al. The NFκB Signaling Pathway in Papillomavirus-induced Lesions: Friend or Foe? Anticancer Res 2016;36:2073-83.
28. Nair A, Venkatraman M, Maliekal TT, et al. NF-kappaB is constitutively activated in high-grade squamous intraepithelial lesions and squamous cell carcinomas of the human uterine cervix. Oncogene 2003;22:50-8.
29. Tilborghs S, Corthouts J, Verhoeven Y, et al. The role of Nuclear Factor-kappa B signaling in human cervical cancer. Crit Rev Oncol Hematol 2017;120:141-50.
30. Kashyap VK, Nagesh PKB, Singh AK, et al. Curcumin attenuates smoking and drinking activated NF-κB/IL-6 inflammatory signaling axis in cervical cancer. Cancer Cell Int 2024;24:343.
31. Lee H, Herrmann A, Deng JH, et al. Persistently activated Stat3 maintains constitutive NF-kappaB activity in tumors. Cancer Cell 2009;15:283-93.
32. Guo C, Qi H, Yu Y, et al. The G-Protein-Coupled Bile Acid Receptor Gpbar1 (TGR5) Inhibits Gastric Inflammation Through Antagonizing NF-κB Signaling Pathway. Front Pharmacol 2015;6:287.
33. Huang X, Wang B, Chen R, et al. The Nuclear Farnesoid X Receptor Reduces p53 Ubiquitination and Inhibits Cervical Cancer Cell Proliferation. Front Cell Dev Biol 2021;9:583146.
34. Huang X, Wang B, Shen H, et al. Farnesoid X receptor functions in cervical cancer via the p14(ARF)-mouse double minute 2-p53 pathway. Mol Biol Rep 2022;49:3617-25.
35. Li YT, Swales KE, Thomas GJ, et al. Farnesoid x receptor ligands inhibit vascular smooth muscle cell inflammation and migration. Arterioscler Thromb Vasc Biol 2007;27:2606-11.
36. Williams TM, Leeth RA, Rothschild DE, et al. The NLRP1 inflammasome attenuates colitis and colitis-associated tumorigenesis. J Immunol 2015;194:3369-80.
37. Bai X, Duan Z, Deng J, et al. Ginsenoside Rh4 inhibits colorectal cancer via the modulation of gut microbiota-mediated bile acid metabolism. J Adv Res 2024. [Epub ahead of print]. doi: 10.1016/j.jare.2024.06.028.
38. DiDonato JA, Hayakawa M, Rothwarf DM, et al. A cytokine-responsive IkappaB kinase that activates the transcription factor NF-kappaB. Nature 1997;388:548-54.
39. Chen ZJ, Parent L, Maniatis T. Site-specific phosphorylation of IkappaBalpha by a novel ubiquitination-dependent protein kinase activity. Cell 1996;84:853-62.
40. Oeckinghaus A, Ghosh S. The NF-kappaB family of transcription factors and its regulation. Cold Spring Harb Perspect Biol 2009;1:a000034.
41. Miyamoto S. Nuclear initiated NF-κB signaling: NEMO and ATM take center stage. Cell Res 2011;21:116-30.
42. Li Z, Yang Z, Lapidus RG, et al. IKK phosphorylation of NF-κB at serine 536 contributes to acquired cisplatin resistance in head and neck squamous cell cancer. Am J Cancer Res 2015;5:3098-110.
43. Arlt A, Bauer I, Schafmayer C, et al. Increased proteasome subunit protein expression and proteasome activity in colon cancer relate to an enhanced activation of nuclear factor E2-related factor 2 (Nrf2). Oncogene 2009;28:3983-96.
44. Kinker GS, Thomas AM, Carvalho VJ, et al. Deletion and low expression of NFKBIA are associated with poor prognosis in lower-grade glioma patients. Sci Rep 2016;6:24160.
45. Nakahara T, Tanaka K, Ohno S, et al. Activation of NF-κB by human papillomavirus 16 E1 limits E1-dependent viral replication through degradation of E1. J Virol 2015;89:5040-59.
46. James MA, Lee JH, Klingelhutz AJ. Human papillomavirus type 16 E6 activates NF-kappaB, induces cIAP-2 expression, and protects against apoptosis in a PDZ binding motif-dependent manner. J Virol 2006;80:5301-7.
47. Chung CH, Lin CY, Chen CY, et al. Ferroptosis Signature Shapes the Immune Profiles to Enhance the Response to Immune Checkpoint Inhibitors in Head and Neck Cancer. Adv Sci (Weinh) 2023;10:e2204514.
48. Anderson KM, Gayer CP. The Pathophysiology of Farnesoid X Receptor (FXR) in the GI Tract: Inflammation, Barrier Function and Innate Immunity. Cells 2021;10:3206.

49. Nevens F, Andreone P, Mazzella G, et al. A Placebo-Controlled Trial of Obeticholic Acid in Primary Biliary Cholangitis. N Engl J Med 2016;375:631-43.
50. Kowdley KV, Luketic V, Chapman R, et al. A randomized trial of obeticholic acid monotherapy in patients with primary biliary cholangitis. Hepatology 2018;67:1890-902.
51. Trauner M, Nevens F, Shiffman ML, et al. Long-term efficacy and safety of obeticholic acid for patients with primary biliary cholangitis: 3-year results of an international open-label extension study. Lancet Gastroenterol Hepatol 2019;4:445-53.
52. Younossi ZM, Ratziu V, Loomba R, et al. Obeticholic acid for the treatment of non-alcoholic steatohepatitis: interim analysis from a multicentre, randomised, placebo-controlled phase 3 trial. Lancet 2019;394:2184-96.
53. Loomba R, Noureddin M, Kowdley KV, et al. Combination Therapies Including Cilofexor and Firsocostat for Bridging Fibrosis and Cirrhosis Attributable to NASH. Hepatology 2021;73:625-43.
54. Sanyal AJ, Lopez P, Lawitz EJ, et al. Tropifexor for nonalcoholic steatohepatitis: an adaptive, randomized, placebo-controlled phase 2a/b trial. Nat Med 2023;29:392-400.
55. Ratziu V, Harrison SA, Loustaud-Ratti V, et al. Hepatic and renal improvements with FXR agonist vonafexor in individuals with suspected fibrotic NASH. J Hepatol 2023;78:479-92.
56. Gadaleta RM, van Erpecum KJ, Oldenburg B, et al. Farnesoid X receptor activation inhibits inflammation and preserves the intestinal barrier in inflammatory bowel disease. Gut 2011;60:463-72.
57. Akwabi-Ameyaw A, Bass JY, Caldwell RD, et al. Conformationally constrained farnesoid X receptor (FXR) agonists: Naphthoic acid-based analogs of GW 4064. Bioorg Med Chem Lett 2008;18:4339-43.
58. Luo G, Lin X, Li Z, et al. Structure-guided modification of isoxazole-type FXR agonists: Identification of a potent and orally bioavailable FXR modulator. Eur J Med Chem 2021;209:112910.
59. Gege C, Kinzel O, Steeneck C, et al. Knocking on FXR's door: the "hammerhead"-structure series of FXR agonists - amphiphilic isoxazoles with potent in vitro and in vivo activities. Curr Top Med Chem 2014;14:2143-58.
60. Bass JY, Caldwell RD, Caravella JA, et al. Substituted isoxazole analogs of farnesoid X receptor (FXR) agonist GW4064. Bioorg Med Chem Lett 2009;19:2969-73.
61. Tully DC, Rucker PV, Chianelli D, et al. Discovery of Tropifexor (LJN452), a Highly Potent Non-bile Acid FXR Agonist for the Treatment of Cholestatic Liver Diseases and Nonalcoholic Steatohepatitis (NASH). J Med Chem 2017;60:9960-73.
62. Guo X, Bian X, Li Y, et al. The intricate dance of tumor evolution: Exploring immune escape, tumor migration, drug resistance, and treatment strategies. Biochim Biophys Acta Mol Basis Dis 2024;1870:167098.
63. Attia YM, Tawfiq RA, Ali AA, et al. The FXR Agonist, Obeticholic Acid, Suppresses HCC Proliferation & Metastasis: Role of IL-6/STAT3 Signalling Pathway. Sci Rep 2017;7:12502.
64. Yu J, Yang K, Zheng J, et al. Activation of FXR and inhibition of EZH2 synergistically inhibit colorectal cancer through cooperatively accelerating FXR nuclear location and upregulating CDX2 expression. Cell Death Dis 2022;13:388.
65. Kao CC, Lai CR, Lin YH, et al. GW4064 inhibits migration and invasion through cathepsin B and MMP2 downregulation in human bladder cancer. Chem Biol Interact 2024;389:110869.

(English Language Editor: L. Huleatt)

Cite this article as: Li Y, Hong Y, Shen H, Zhou J, Cesar D, Eleutério J Jr, Matsuura M, Liu Y, Luo C, Li Q. FXR activation suppresses NF-κB signaling, proliferation and migration in cervical cancer cells. Transl Cancer Res 2025;14(4):2440-2456. doi: 10.21037/tcr-2025-522